Biochemical and Biophysical Research Communications 411 (2011) 190–196

Contents lists available at ScienceDirect

Biochemical and Biophysical Research Communications

journal homepage: www.elsevier.com/locate/ybbrc

Single particle analysis of tau oligomer formation induced by metal ions and organic solvents

Benedikt Bader [a,b,1], Georg Nübling [a,b,1], Anja Mehle [a], Simona Nobile [a], Hans Kretzschmar [a], Armin Giese [a,*]

[a] Zentrum für Neuropathologie und Prionforschung, Ludwig-Maximilians-Universität, München, Germany
[b] Neurologische Klinik und Poliklinik, Klinikum der Universität München, Germany

ARTICLE INFO

Article history:
Received 14 June 2011
Available online 24 June 2011

Keywords:
Tau
Alpha-synuclein
Neurodegeneration
Dementia
Alzheimer
Oligomer
Fluorescence correlation spectroscopy

ABSTRACT

Pathological aggregates of tau protein are found in several neurodegenerative diseases termed 'tauopathies'. Increasing evidence indicates that tau oligomer species rather than the large amyloid cytoplasmic inclusions relevant for histopathological diagnosis might be crucial for cellular damage and neurodegeneration. Trivalent metal ions and polyanionic structures like heparin or arachidonic acid have been shown to induce tau aggregation. However, little is known about early processes of tau aggregation. In this study, we applied fluorescence correlation spectroscopy (FCS) and scanning for intensely fluorescent targets (SIFT) to investigate oligomer formation of tau protein at nanomolar protein concentrations at the single-particle level. Our results indicate that the formation of distinct tau oligomers is induced by the trivalent metal ions Fe^{3+} and Al^{3+} and by organic solvents like DMSO, respectively. In contrast, bivalent metal ions (Cu^{2+}, Zn^{2+}, Mn^{2+}, Ca^{2+}, Mg^{2+}) had no effect. While DMSO-induced small tau oligomers are relatively stable in solution, dynamic remodeling can be initiated by non-ionic detergents. Moreover Al^{3+} induces rapid formation of a different oligomer species of larger size. Our results provide further insights into early tau oligomerization and aggregation dynamics.

1. Introduction

Deposits of tau protein are histopathologic hallmarks of several neurodegenerative diseases termed 'tauopathies', including Alzheimer's disease and fronto-temporal lobar degeneration with tau inclusions (FTLD-tau) [1,2]. In these diseases, large aggregates of tau form distinct structures like neurofibrillary tangles (NFT), neuropil threads and glial inclusions. While these aggregates are suitable for histopathological diagnosis and correlate with disease progression [3], they are preceded by smaller oligomers. However, it is still unclear how these oligomer species contribute to neurotoxicity. Increasing evidence indicates that oligomers are the pathophysiologically relevant species [4–6]. Tau over-expression proved to be toxic to cells before the appearance of NFTs in a transgenic *Drosophila* model [4]. In a mouse model of inducible tauopathy, blockage of tau over-expression alleviated cognitive dysfunction even after the appearance of NFTs. Interestingly, cognitive dysfunction improved even though the level of NFTs increased. This indicates that not amyloid aggregates but another species exerts toxicity [5].

In aqueous solution, high protein concentration is required for tau aggregation into amyloid fibers in the absence of aggregation inducers [7]. Thus, polyanions like heparin and arachidonic acid (ARA) are used in *in vitro* models to induce the formation of Thioflavin positive amyloid tau aggregates strongly resembling Alzheimer PHFs [8–11]. To induce tau aggregation, ARA has to be present in concentrations exceeding its critical micelle concentration, providing a polyanionic micellar surface [9,12]. In general, organic solvents are used to increase solubility of ARA in aqueous solutions, and thus a pro-aggregatory influence of organic solvents has to be considered. It is known that organic solvents mimic perimembranous conditions by reducing the dielectric constant [13], which might be relevant since it was shown that large tau aggregates may originate from intracellular membranes [14,15]. Other models of tau aggregation uses trivalent metal ions like Fe^{3+} and Al^{3+}. Especially aluminium has been extensively investigated, since early studies on rabbit brains showed the formation of NFT-like structures after intrathecal injection of aluminium [16]. However, numerous *in vitro*, *in vivo* and epidemiological studies could not elucidate the pathophysiologic significance of aluminium in AD and other tauopathies [17,18]. In this study, we applied fluorescence correlation spectroscopy (FCS) and scanning for intensely fluorescent targets (SIFT) to investigate early aggregation steps of tau protein at nanomolar concentrations. These techniques are suitable to detect femtomolar concentrations of fluorescently labeled aggregates [19].

* Corresponding author. Address: Zentrum für Neuropathologie und Prionforschung, Ludwig-Maximilians-Universität, Feodor-Lynen-Str. 23, 81377 München, Germany. Fax: +49 (0)89 218078037.
E-mail address: armin.giese@med.uni-muenchen.de (A. Giese).
[1] These authors contributed equally.

0006-291X/$ - see front matter © 2011 Elsevier Inc. All rights reserved.
doi:10.1016/j.bbrc.2011.06.135

Although extensive investigations on the aggregation behavior of tau under different conditions have been conducted, little is known about early steps of tau oligomerization. Established techniques like Thioflavin T are able to sensitively quantify amyloid-like aggregates, but are of limited use in studying oligomer properties. Other techniques like atomic force microscopy are suitable to examine the structure of large fibrils as well as smaller oligomers, but comprise difficulties in quantification and cannot investigate oligomerization dynamics. We investigated the influence of the organic solvent dimethylsulfoxide (DMSO), trivalent and divalent metal ions on tau aggregation, and the dynamics of pre-formed, DMSO-induced oligomers.

2. Materials and methods

2.1. Proteins

Tau isoforms htau37 (1N3R) and htau46 (1N4R) were expressed in *Escherichia coli* BL21 (DE3) RIL and purified by sterile filtration, cation exchange chromatography and ammonium salt precipitation. The plasmid was a gift of Manuela Neumann (ZNP Munich/Zurich). Cultures were transformed and cultivated in rich LB medium and lysed using a French press. Protease inhibitor Complete Mini (Roche, Germany) was added, the lysate was centrifuged at 27,000*g* and the supernatant was filtered using a 0.45 μm sterile filtropur S-filter (Sarstedt, Germany). The filtrate was loaded on a P11 phosphocellulose cation exchange column and the protein was eluted using a 100–300 mM NaCl gradient on an Äkta Prime FPLC-device (Amersham, Germany). Fractions containing high amounts of tau were identified by Western blot using T46 antibody (Zymed/Invitrogen, Germany) and precipitated by $(NH_4)_2SO_4$. The precipitated solution was incubated for 10 min at 95 °C and a buffer exchange to 50 mM Tris, pH 7.0 was performed using a PD10 desalting column (Amersham). Alpha-synuclein (α-syn) was produced according to established protocols [20]. A stock solution containing 1 mg/ml α-syn was prepared in 50 mM Tris buffer, pH 7.0. Bovine serum albumin (BSA) (Sigma Aldrich, Germany) was used as control.

2.2. Confocal single particle analysis

FCS, FIDA, and SIFT were performed on an Insight Reader (Evotec-Technologies, Hamburg, Germany) with dual-color excitation (488 and 633 nm) as described previously [21]. Photon intensities (*I*) were collected separately for two emission wavelength ranges (green (*Ig*) and red (*Ir*)) by single-photon detectors and analyzed using FCSPP software version 2.0, FIDA-Analyze software, and SIFT-2D (Evotec-Technologies).

For SIFT-2D analysis, photons were added in time intervals (bins) of 40 μs in a 2D intensity histogram ($H_{Ig,Ir}$). For each analysis, a threshold (*T*) was determined in calibration measurements to define the cut-off level between monomers and multimers. For bin-weighted SIFT analyses, all high-intense bins (*N*) correspond to the sum of all frequencies $h_{Ig,Ir}$ with $(Ig^2 + Ir^2 \geqslant T^2)$. In some cases, photon-weighted SIFT analysis was used with P = sum of all $h_{Ig,Ir} * (Ig + Ir)$ with $(Ig^2 + Ir^2 \geqslant T^2)$. Dual-color aggregates are defined as high-intensity signal $(Ig^2 + Ir^2 \geqslant T^2)$ with Ig/Ir and $Ir/Ig > 1/6$. In fluorescence intensity distribution analysis (FIDA), the brightness (*Q*) of component 1 (*Q*1) and component 2 (*Q*2) were determined by software fit. To calculate the approximate particle size, particle brightness of aggregate species (*Q*2) was divided by the particle brightness of monomers (*Q*1). After addition of NP40 or Al^{3+}, values of the steady-state-phase between minute 280 and 360 of oligomer formation were averaged.

2.3. Protein labeling

For single molecule analysis, proteins were labeled with fluorescent dyes Alexa-488-O-succiminidylester or Alexa-647-O-succiminidylester as described previously [21]. Tau protein and BSA were incubated with a fourfold molar excess of fluorescent dye in 100 mM $NaHCO_3$ for 24 h at room temperature. For α-syn, a twofold molar excess was used. Unbound dye was separated using a PD10 desalting column (GE Healthcare, Germany). Absence of unbound dye and the labeling ratio (dye/protein) was confirmed by FCS measurements. Labeled proteins are further referred to as tau-488, tau-647, α-syn-488, α-syn-647, BSA-488 and BSA-647, respectively.

2.4. Aggregation assay

Fivefold stock solutions of labeled proteins were prepared to reach a final concentration of 5 molecules per focal volume per detection channel, equivalent to a concentration of 10 nM. For tau aggregation experiments, stock solutions were centrifuged at 100,000*g* for 30 min to remove pre-formed aggregates (see Supplementary Fig. 1). Absence of pre-formed aggregates was confirmed by SIFT [21]. Only samples free of pre-formed aggregates were used and experiments were started immediately. All experiments were conducted in 96-well cover slide bottom plates in a volume of 20 μl per well. Plates were covered with adhesive film to prevent evaporation. For aggregation experiments, protein stock solutions were added to wells containing 50 mM Tris buffer and measurements were started immediately. If not otherwise specified, a final concentration of 10 μM was used for $AlCl_3$, $FeCl_3$, $CuCl_2$, $MnCl_2$, $ZnCl_2$, $CaCl_2$ and $MgCl_2$. Final concentrations were 1% for DMSO and 0.1% of nonident P40 (NP40) if not stated otherwise. Concentrations of sodium dodecylsulfate (SDS) are given in the respective experiments.

3. Results

3.1. Establishing a single molecule tau aggregation assay

To sensitively detect *de novo* protein oligomerization, the aggregation assay must be free of pre-formed aggregates that might have a seeding effect on aggregation [22]. We evaluated different approaches to remove pre-existing aggregates of fluorescent labeled tau. Sonication does not remove pre-formed aggregates. After ultracentrifugation, the majority of tau oligomers are detected in the pellet while the aggregate contamination of the supernatant is low (Supplementary Fig. 1A and B). All further experiments were thus conducted after ultracentrifugation of tau stock solutions.

3.2. Tau aggregation induced by organic solvents and detergents

It has been shown that organic solvents mimic a perimembranous environment, induce conformational changes in tau protein [23,24] and promote protein aggregation [13,20]. In our experiments, DMSO at a final concentration of ⩾1% induces the formation of protein oligomers, resembling the effect on α-syn aggregation described previously (Fig. 1A and B) [20]. Interestingly, SIFT-2D analysis indicates comparable sizes of DMSO-induced tau and α-syn oligomers (Fig. 1A). While the non-ionic detergent NP40 efficiently inhibits the formation of DMSO induced α-syn aggregates, it has a positive effect on tau aggregation compared to control measurements without inducers. No significant differences are seen in the behavior of three and four repeat tau (1N3R, 1N4R) under these conditions (Supplementary Fig. 2). As a control protein

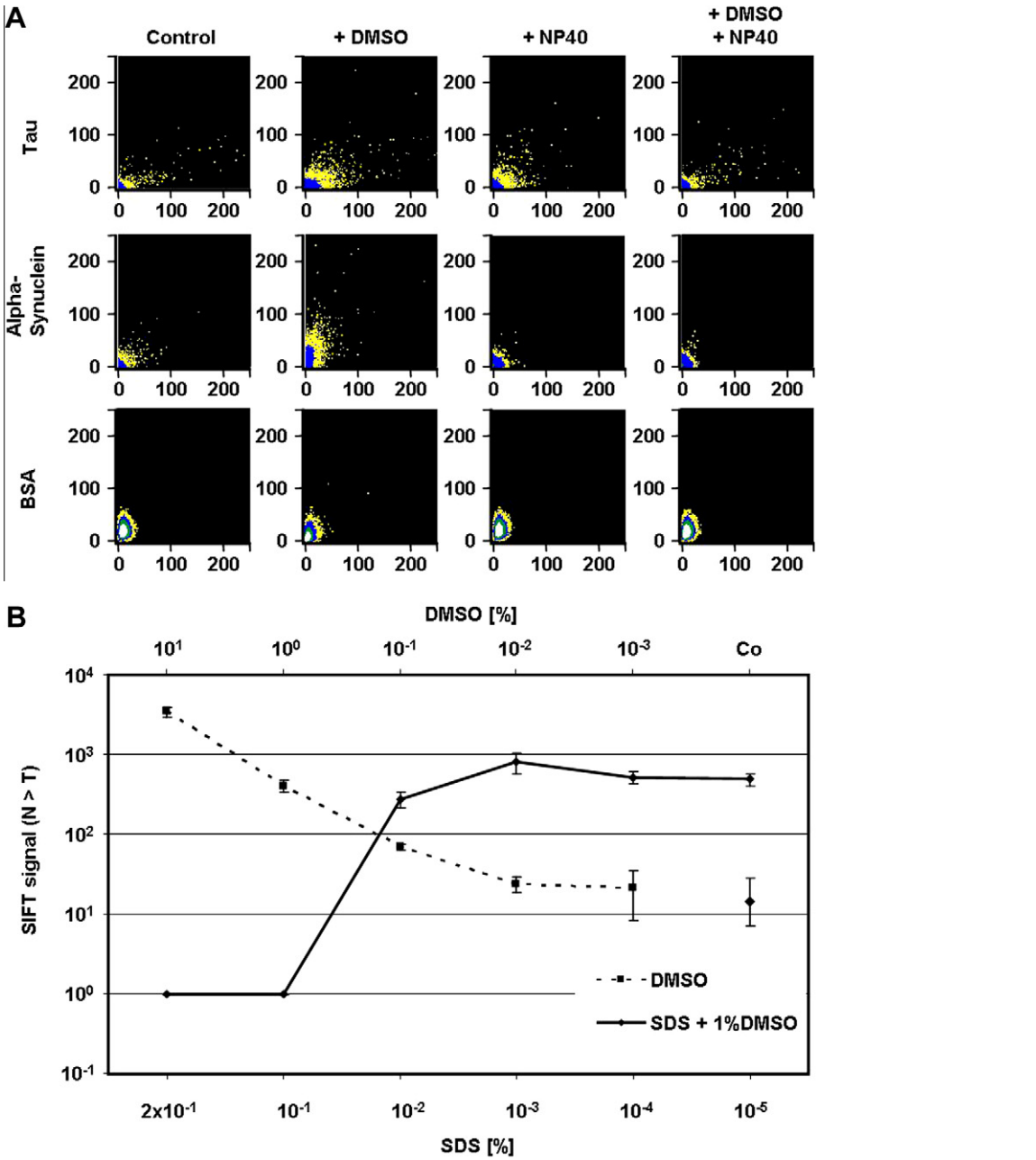

Fig. 1. Tau aggregation in presence of organic solvents and detergent. (A) DMSO induces the formation of small tau and α-syn oligomers, but has no effect on BSA. Whereas no α-syn aggregates form in presence of NP40, it induces tau oligomer formation. (B) DMSO shows a dose dependent induction of tau aggregation. SDS counteracts the pro-aggregatory effect of 1% DMSO at concentrations >0.01%. Co: control (♦) without addition of DMSO or SDS. Error bars indicate standard deviation of four parallel experiments.

unrelated to neurodegenerative protein aggregation diseases, BSA does not show any aggregation tendency, neither in presence of DMSO nor NP40 (Fig. 1A). The ionic detergent SDS counteracts the pro-aggregatory effect of 1% DMSO on tau at concentrations above 0.01% (Fig. 1B). However, lower concentrations of SDS do not inhibit DMSO-induced tau aggregation.

3.3. Tau aggregation induced by metal ions

Numerous studies demonstrated that metal ions can induce the formation of large tau aggregates detectable by electron microscopy [17,25,26].

In our assay, the trivalent metal ions Al^{3+} and Fe^{3+} induce the formation of tau aggregates in a dose-dependent manner at concentrations of $\geqslant 3$ μM. At 10 μM, Fe^{3+} and Al^{3+} show a strong pro-aggregatory effect compared to controls. Interestingly, aggregates formed in presence of Fe^{3+} demonstrate a shift to the red fluorescence (Fig. 2A), even though tau-647 and tau-488 are present in equal ratios as determined by evaluation of brightness and particle concentration in the green and red channel prior to each experiment (data not shown). As all components of the assay, 10 μM Fe^{3+} did not show auto-fluorescence in a control experiment (data not shown). SIFT-2D analysis indicates the formation of distinct oligomer species for Al^{3+} and Fe^{3+}, which are larger than DMSO-induced oligomers.

Moreover, we examined the influence of the bivalent metal ions Ca^{2+}, Cu^{2+}, Mn^{2+}, Mg^{2+} and Zn^{2+} on tau aggregation. None of these ions showed a significant influence on tau aggregation at a final concentration of 10 μM (Fig. 2A). In summary, our data demonstrate that trivalent, but not bivalent metal ions show a strong

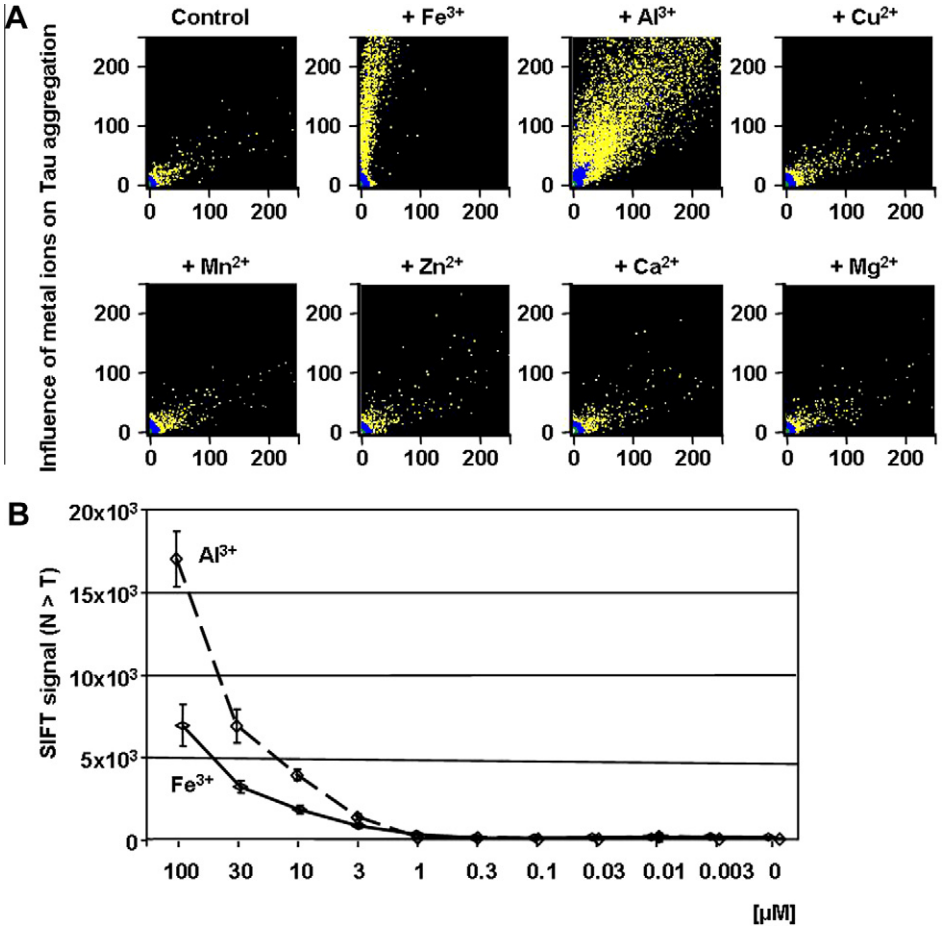

Fig. 2. Influence of metal ions on tau aggregation. (A) SIFT-2D analysis shows the formation of distinct oligomers in presence of Fe^{3+} and Al^{3+} at 10 µM. The bivalent metal ions Cu^{2+}, Mn^{2+}, Zn^{2+}, Ca^{2+} and Mg^{2+} have no influence on aggregation. (B) Both Fe^{3+} and Al^{3+} induce aggregation in a dose-dependent manner. Concentrations below 1 µM show no influence. Error bars indicate standard deviation of four parallel experiments.

effect on tau aggregation in our assay conditions, and that the resulting oligomers differ in size from DMSO-induced oligomers.

3.4. Investigation of tau oligomer dynamics

To elucidate the dynamics of association and dissociation of tau oligomers in aqueous solution, tau-488 and tau-647 were incubated separately with 1% DMSO for 90 min. Subsequently, pre-formed single-color tau oligomers were mixed, and analyzed for another 4 h (Fig. 3A). SIFT analysis was used to distinguish between single-color and dual-color oligomers. In these experiments, the amount of dual-color aggregates is stable at approximately 25% of total aggregates, proving high stability of the pre-formed single-color oligomers (Fig. 3B). Furthermore, aggregate size as determined by particle brightness (Q2) in a two-component FIDA fit also remains stable (mean: 63 monomers/oligomer). After 4 h, either 0.1% NP40 or 10 µM Al^{3+} was added to the assay. Upon addition of NP40, a gradual shift towards dual-color aggregate formation is demonstrated, with a stable level of 60–70% reached after 30–60 min (Fig. 3B). The average size of aggregates formed after addition of NP40 is smaller than of the pre-formed DMSO aggregates (mean: 34 monomers/oligomer). Upon addition of Al^{3+}, large dual-color aggregates are formed rapidly. These aggregates reach more than fourfold the brightness of DMSO-induced aggregates within 30 min (mean: 370 monomers/oligomer), and the percentage of dual-color aggregates reaches almost 100% (Fig. 3C). In summary, DMSO-induced aggregates are stable over time and dynamic remodeling of tau oligomers can be induced by non-ionic detergents like NP40 and trivalent metal ions like Al^{3+}.

4. Discussion

Numerous studies investigated the influence of metal ions and membrane surfaces in the form of polyanionic micelles on tau aggregation [10,17,26]. However, little is known about early aggregation processes. In this study, we developed a *de novo* aggregation assay to investigate early oligomerization of tau at the single-molecule level, using organic solvents and metal ions as oligomerization inducers. The main methods in our study, FCS and SIFT, use nanomolar protein concentrations and can detect femtomolar concentrations of aggregates [19,27]. Although the precise cytoplasmatic concentration of monomeric tau in early stages of neurodegeneration is unknown, the concentration used in our assay might better depict physiological intracellular conditions of free monomeric tau in early stages of neurodegeneration than commonly used assays of tau fibrillization.

4.1. Organic solvents induce tau oligomerization

Based on the observation that PHFs might originate from intracellular membranes, the influence of polyanionic membrane surfaces on tau aggregation has long been discussed [14,15]. To determine whether membrane surfaces can induce tau aggregation, various fatty acids were investigated concerning their potential as aggregation inducers [10]. It was demonstrated that

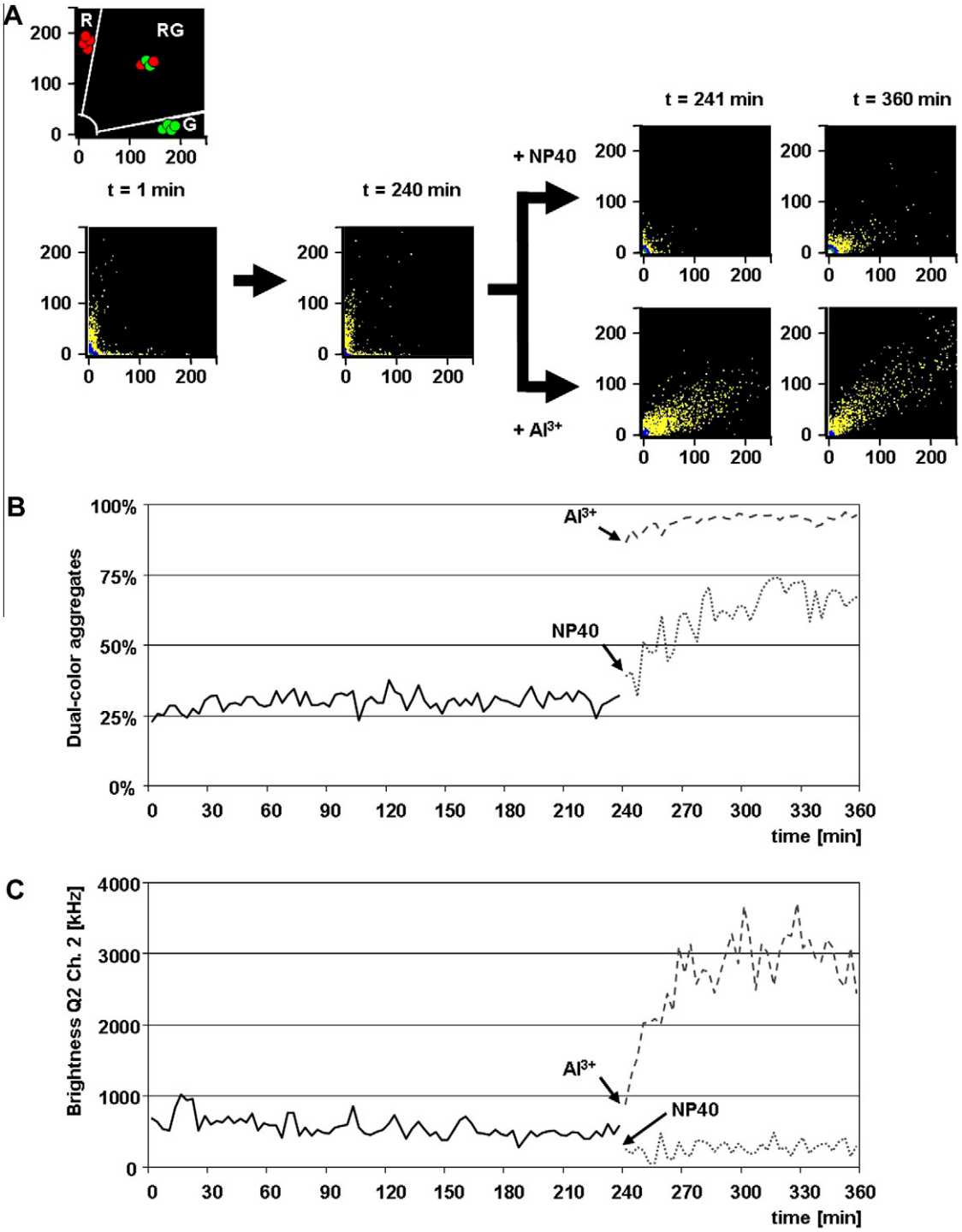

Fig. 3. Investigation of oligomer dynamics. Tau-488 and tau-647 were incubated in presence of 1% DMSO for 90 min. Both solutions were combined (t = 1 min) and measurements were continued for 4 h, showing mainly single-color aggregates (sectors R and G) and only a low rate of dual-color aggregates (sector RG). While the number of dual-color aggregates increases slowly after addition of NP40, large dual-color aggregates form immediately after addition of Al^{3+}. (C) Aggregates formed in presence of 1% DMSO are stable in regard to size as demonstrated by stable particle brightness (Q2) (red channel shown). Oligomers formed in presence of Al^{3+} exceed DMSO-induced aggregate size while aggregates formed in presence of NP40 are smaller than oligomers formed in DMSO. (For interpretation of the references to color in this figure legend, the reader is referred to the web version of this article.)

polyanionic micelles induce rapid formation of Thioflavin-positive aggregates [9,10]. Furthermore, electron microscopy studies suggested that tau fibrils may directly originate from these micelles [10]. Organic solvents alter the dielectric constant of aqueous solutions mimicking a perimembranous environment [13]. It was shown before that organic solvents alter the conformational status of tau and may have an intrinsic pro-aggregatory influence [23,24]. Therefore, organic solvents may serve as an interesting *in vitro* model to study early tau aggregation processes.

In our experiments, DMSO induces the formation of small oligomers in a dose-dependent matter. This process appears to be specific for amyloidogenic proteins, since it could not be

reproduced with BSA as a control protein. Interestingly, the pro-aggregatory effect of DMSO can be abolished by addition of the ionic detergent SDS. Since SDS denatures secondary and tertiary protein structure [28], this might indicate that tau aggregation is triggered by conformational changes induced by DMSO.

When single-color DMSO-induced tau-488 oligomers are co-incubated with single-color tau-647 oligomers, the number of newly emerging dual-color aggregates remains low. We reason that this indicates a very low intrinsic turn-over rate (i.e. association and dissociation of monomers to/from oligomers) once oligomers have been formed. Upon addition of the non-ionic detergent NP40, the number of dual-color aggregates increased over 30–60 min reaching a stable maximum of 60–70% of all aggregates. This indicates an increased turnover of tau oligomers. It has to be discussed that turnover of tau oligomers formed in a cellular environment is significantly influenced by interacting factors in a similar way as by detergents such as NP40. However, at this stage we can only speculate on how these oligomers contribute to tau pathology, and whether they represent an early step on the pathway to large amyloid aggregates.

4.2. Influence of metal ions on tau aggregation

The influence of metal ions, especially of aluminium, on the aggregation behavior of tau has been extensively studied since Klatzo et al. identified NFT-like structures in rabbit brains after injection of aluminium [16]. However, a vast number of *in vitro*, *in vivo* and epidemiological studies were so far unable to consistently determine the pathophysiological relevance of aluminium in Alzheimer's disease and other tauopathies [18]. Numerous studies demonstrated that Al^{3+} induces the formation of tau aggregates that appear to be off pathway to fibrillization, since only amorphous aggregates were seen repeatedly in electron microscopy [25,26,29]. Similar data was published for Fe^{3+} [26].

However, it has to be considered that the methods commonly used to study tau aggregation typically employ high concentrations of both protein and inducer which might not depict the physiological situation in the cytoplasm. For example, several studies investigating the effect of Al^{3+} applied millimolar concentrations of the metal ion, even though studies on post-mortem brain tissues rarely find concentrations exceeding 60 μmol/kg (wet weight) [30–32]. In our assay, we show that Al^{3+} and Fe^{3+} at final concentrations of 10 μM induce the formation of distinct tau oligomers, demonstrating that even physiological concentrations of these metal ions may influence tau pathology.

A possible role of metal ion-induced protein aggregates is also supported by studies on α-syn, where Fe^{3+} induces the formation of α-syn oligomers with pore-forming abilities [20]. If Fe^{3+} leads to toxic pore formation, comparable effects might be relevant for other amyloidogenic proteins.

In our study, only the trivalent metal ions Al^{3+} and Fe^{3+} induced a rapid, dose-dependent formation of large tau oligomers. Our experiments on oligomer dynamics suggest that Al^{3+} induces aggregation of both tau monomers and oligomers since the ratio of dual-color aggregates in the steady state phase is close to 100% even if pre-formed single-color DMSO-induced oligomers are present before addition of Al^{3+}. Thus, either single-color oligomers were rapidly dissolved and rebuilt into new aggregates, or existing aggregates are combined to larger aggregates. We suggest the latter to be more likely, since this process is extremely rapid compared to detergent-induced oligomer remodeling (Fig. 3B). The finding that both Al^{3+} and Fe^{3+} induce formation of large tau oligomers argues that this effect is not mediated by redox reactions but by formation of protein/metal ion complexes. Interestingly, aggregation induced by 10 μM Al^{3+} reached a steady state after 30 min, and 1 μM Al^{3+} or 1 μM Fe^{3+} only had a mild effect on tau aggregation. These findings indicate that a certain molar excess of trivalent metal ions is required to induce tau aggregation.

The actual size of dual-color aggregates can be calculated by dividing the particle brightness of aggregates by the particle brightness of the monomer in the green and red channel. Interestingly, aggregates induced by NP40 on average consist of 34 monomers, while those induced by DMSO on average comprise 63 monomers. Aggregates induced by Al^{3+} are much larger (mean: 370 monomers). Since the oligomer sizes in the presence of NP40 and Al^{3+} reach a steady state, it can be speculated that the oligomer architecture is specific for the respective inducer.

In conclusion, our data demonstrate that both organic solvents and the trivalent metal ions Al^{3+} and Fe^{3+} induce the formation of distinct tau oligomer species and shed light on tau oligomer dynamics. The *de novo* aggregation assay presented here may prove to be a powerful tool to further investigate various aspects of early tau oligomerization. More detailed work is required to further characterize tau oligomers and to determine possible mechanisms of cellular toxicity and their role in the pathophysiology of tauopathies. Future studies may investigate the influence of post-translational modifications like phosphorylation and limited proteolysis on tau aggregation. The assay also allows high-throughput screening of aggregation inhibitors, as was demonstrated before for prion protein [33]. Furthermore, dual-color experiments could be used to evaluate co-aggregation processes between tau protein and other proteins such as α-syn which are involved in neurodegenerative diseases, as the issue of co-aggregation and cross-seeding of disease-specific proteins recently gained scientific interest [1].

Acknowledgments

The authors thank Manuela Neumann and Ben Vanmassehove for their support of these studies. This work was supported by SFB-Grant 596-B13 to A.G. and H.K.

Appendix A. Supplementary data

Supplementary data associated with this article can be found, in the online version, at doi:10.1016/j.bbrc.2011.06.135.

References

[1] W.R. Galpern, A.E. Lang, Interface between tauopathies and synucleinopathies: a tale of two proteins, Ann. Neurol. 59 (2006) 449–458.
[2] I.R. Mackenzie, M. Neumann, E.H. Bigio, N.J. Cairns, I. Alafuzoff, J. Kril, G.G. Kovacs, B. Ghetti, G. Halliday, I.E. Holm, P.G. Ince, W. Kamphorst, T. Revesz, A.J. Rozemuller, S. Kumar-Singh, H. Akiyama, A. Baborie, S. Spina, D.W. Dickson, J.Q. Trojanowski, D.M. Mann, Nomenclature and nosology for neuropathologic subtypes of frontotemporal lobar degeneration: an update, Acta Neuropathol. 119 (2010) 1–4.
[3] H. Braak, I. Alafuzoff, T. Arzberger, H.A. Kretzschmar, K. Del Tredici, Staging of Alzheimer disease-associated neurofibrillary pathology using paraffin sections and immunocytochemistry, Acta Neuropathol. 112 (2006) 389–404.
[4] C.W. Wittmann, M.F. Wszolek, J.M. Shulman, P.M. Salvaterra, J. Lewis, M. Hutton, M.B. Feany, Tauopathy in *Drosophila*: neurodegeneration without neurofibrillary tangles, Science 293 (2001) 711–714.
[5] K. Santacruz, J. Lewis, T. Spires, J. Paulson, L. Kotilinek, M. Ingelsson, A. Guimaraes, M. DeTure, M. Ramsden, E. McGowan, C. Forster, M. Yue, J. Orne, C. Janus, A. Mariash, M. Kuskowski, B. Hyman, M. Hutton, K.H. Ashe, Tau suppression in a neurodegenerative mouse model improves memory function, Science 309 (2005) 476–481.
[6] Y. Yoshiyama, M. Higuchi, B. Zhang, S.M. Huang, N. Iwata, T.C. Saido, J. Maeda, T. Suhara, J.Q. Trojanowski, V.M. Lee, Synapse loss and microglial activation precede tangles in a P301S tauopathy mouse model, Neuron 53 (2007) 337–351.
[7] H. Wille, G. Drewes, J. Biernat, E.M. Mandelkow, E. Mandelkow, Alzheimer-like paired helical filaments and antiparallel dimers formed from microtubule-associated protein tau in vitro, J. Cell Biol. 118 (1992) 573–584.
[8] M.E. King, T.C. Gamblin, J. Kuret, L.I. Binder, Differential assembly of human tau isoforms in the presence of arachidonic acid, J. Neurochem. 74 (2000) 1749–1757.
[9] S. Barghorn, E. Mandelkow, Toward a unified scheme for the aggregation of tau into Alzheimer paired helical filaments, Biochemistry 41 (2002) 14885–14896.

[10] C.N. Chirita, M. Necula, J. Kuret, Anionic micelles and vesicles induce tau fibrillization in vitro, J. Biol. Chem. 278 (2003) 25644–25650.
[11] N. Sahara, S. Maeda, M. Murayama, T. Suzuki, N. Dohmae, S.H. Yen, A. Takashima, Assembly of two distinct dimers and higher-order oligomers from full-length tau, Eur. J. Neurosci. 25 (2007) 3020–3029.
[12] M.E. King, V. Ahuja, L.I. Binder, J. Kuret, Ligand-dependent tau filament formation: implications for Alzheimer's disease progression, Biochemistry 38 (1999) 14851–14859.
[13] L.A. Munishkina, C. Phelan, V.N. Uversky, A.L. Fink, Conformational behavior and aggregation of alpha-synuclein in organic solvents: modeling the effects of membranes, Biochemistry 42 (2003) 2720–2730.
[14] E.G. Gray, M. Paula-Barbosa, A. Roher, Alzheimer's disease: paired helical filaments and cytomembranes, Neuropathol. Appl. Neurobiol. 13 (1987) 91–110.
[15] W. Bondareff, S.S. Matsuyama, P. Dell'Albani, Production of paired helical filament, tau-like proteins by PC12 cells: a model of neurofibrillary degeneration, J. Neurosci. Res. 52 (1998) 498–504.
[16] I. Klatzo, H. Wisniewski, E. Streicher, Experimental production of neurofibrillary degeneration. I. Light microscopic observations, J. Neuropathol. Exp. Neurol. 24 (1965) 187–199.
[17] T. Mizoroki, S. Meshitsuka, S. Maeda, M. Murayama, N. Sahara, A. Takashima, Aluminum induces tau aggregation in vitro but not in vivo, J. Alzheimers Dis. 11 (2007) 419–427.
[18] D. Krewski, R.A. Yokel, E. Nieboer, D. Borchelt, J. Cohen, J. Harry, S. Kacew, J. Lindsay, A.M. Mahfouz, V. Rondeau, Human health risk assessment for aluminium, aluminium oxide, and aluminium hydroxide, J. Toxicol. Environ. Health B. Crit. Rev. 10 (Suppl. 1) (2007) 1–269.
[19] J. Bieschke, A. Giese, W. Schulz-Schaeffer, I. Zerr, S. Poser, M. Eigen, H.A. Kretzschmar, Ultrasensitive detection of pathological prion protein aggregates by dual-color scanning for intensely fluorescent targets, Proc. Natl. Acad. Sci. USA 97 (2000) 5468–5473.
[20] M. Kostka, T. Hogen, K.M. Danzer, J. Levin, M. Habeck, A. Wirth, R. Wagner, C.G. Glabe, S. Finger, U. Heinzelmann, P. Garidel, W. Duan, C.A. Ross, H.A. Kretzschmar, A. Giese, Single particle characterization of iron-induced pore-forming alpha-synuclein oligomers, J. Biol. Chem. 283 (2008) 10992–11003.
[21] A. Giese, B. Bader, J. Bieschke, G. Schaffar, S. Odoy, P.J. Kahle, C. Haass, H. Kretzschmar, Single particle detection and characterization of synuclein co-aggregation, Biochem. Biophys. Res. Commun. 333 (2005) 1202–1210.
[22] J.D. Harper, P.T. Lansbury Jr., Models of amyloid seeding in Alzheimer's disease and scrapie: mechanistic truths and physiological consequences of the time-dependent solubility of amyloid proteins, Annu. Rev. Biochem. 66 (1997) 385–407.
[23] S. Hiraoka, T.M. Yao, K. Minoura, K. Tomoo, M. Sumida, T. Taniguchi, T. Ishida, Conformational transition state is responsible for assembly of microtubule-binding domain of tau protein, Biochem. Biophys. Res. Commun. 315 (2004) 659–663.
[24] K. Minoura, F. Mizushima, M. Tokimasa, S. Hiraoka, K. Tomoo, M. Sumida, T. Taniguchi, T. Ishida, Structural evaluation of conformational transition state responsible for self-assembly of tau microtubule-binding domain, Biochem. Biophys. Res. Commun. 327 (2005) 1100–1104.
[25] C.W. Scott, A. Fieles, L.A. Sygowski, C.B. Caputo, Aggregation of tau protein by aluminum, Brain Res. 628 (1993) 77–84.
[26] A. Yamamoto, R.W. Shin, K. Hasegawa, H. Naiki, H. Sato, F. Yoshimasu, T. Kitamoto, Iron (III) induces aggregation of hyperphosphorylated tau and its reduction to iron (II) reverses the aggregation: implications in the formation of neurofibrillary tangles of Alzheimer's disease, J. Neurochem. 82 (2002) 1137–1147.
[27] J. Levin, U. Bertsch, H. Kretzschmar, A. Giese, Single particle analysis of manganese-induced prion protein aggregates, Biochem. Biophys. Res. Commun. 329 (2005) 1200–1207.
[28] D. Otzen, Protein–surfactant interactions: a tale of many tales, Biochim. Biophys. Acta 1814 (2011) 562–591.
[29] W. Li, K.K. Ma, W. Sun, H.K. Paudel, Phosphorylation sensitizes microtubule-associated protein tau to Al(3+)-induced aggregation, Neurochem. Res. 23 (1998) 1467–1476.
[30] J.R. McDermott, A.I. Smith, K. Iqbal, H.M. Wisniewski, Brain aluminum in aging and Alzheimer disease, Neurology 29 (1979) 809–814.
[31] W.R. Markesbery, W.D. Ehmann, M. Alauddin, T.I. Hossain, Brain trace element concentrations in aging, Neurobiol. Aging 5 (1984) 19–28.
[32] E. Andrasi, N. Pali, Z. Molnar, S. Kosel, Brain aluminum, magnesium and phosphorus contents of control and Alzheimer-diseased patients, J. Alzheimers Dis. 7 (2005) 273–284.
[33] U. Bertsch, K.F. Winklhofer, T. Hirschberger, J. Bieschke, P. Weber, F.U. Hartl, P. Tavan, J. Tatzelt, H.A. Kretzschmar, A. Giese, Systematic identification of antiprion drugs by high-throughput screening based on scanning for intensely fluorescent targets, J. Virol. 79 (2005) 7785–7791.